Deep-Time Marine Sedimentary Element Database

Jiankang Lai[1], Haijun Song[1*], Daoliang Chu[1], Jacopo Dal Corso[1], Erik A. Sperling[2], Yuyang Wu[1*], Xiaokang Liu[1], Lai Wei[3], Mingtao Li[4], Hanchen Song[1], Yong Du[1], Enhao Jia[1], Yan Feng[1], Huyue Song[1], Wenchao Yu[1], Qingzhong Liang[5], Xinchuan Li[5], Hong Yao[5]

[1]State Key Laboratory of Biogeology and Environmental Geology, School of Earth Sciences, China University of Geosciences, Wuhan 430074, China

[2]Department of Earth and Planetary Sciences, Stanford University, Stanford, CA 94305, USA.

[3]School of Future Technology, China University of Geosciences, Wuhan 430074, China

[4]School of Resources and Environment, Linyi University, Linyi 276000, China

[5]School of Computer Science, China University of Geosciences, Wuhan 430074, China

Corresponding authors: Haijun Song (haijunsong@cug.edu.cn), Yuyang Wu (wuyuyang@cug.edu.cn)

Abstract. Geochemical data from ancient marine sediments are crucial to study palaeoenvironments, palaeoclimates, and elemental cycles. With increased accessibility to geochemical data, many databases have emerged. However, there remains a need for a more comprehensive database that focuses on deep-time marine sediment records. Here, we introduce the "Deep-Time Marine Sedimentary Element Database" (DM-SED). The DM-SED has been built upon the "Sedimentary Geochemistry and Paleoenvironments Project" (SGP) database with the new compilation of 34,874 data entries from 433 studies, totalling 63,627 entries. The DM-SED contains 2,522,255 discrete marine sedimentary data points, including major and trace elements and some stable isotopes. It includes 9,207 entries from the Precambrian and 54,420 entries from the Phanerozoic, thus providing significant references for reconstructing deep-time Earth system evolution. The data files described in this paper are available at https://doi.org/10.5281/zenodo.14771859 (Lai et al., 2025).

1 Introduction

Geochemical data from deep-time marine sediments are fundamental for reconstructing the evolution of the Earth system. By analysing the content of chemical elements in sediments and their isotopic compositions, we can reconstruct the past cycling of elements in the Earth's surface systems and reveal the evolution of Earth's surface systems through time (Large et al., 2015; Reinhard et al., 2017; Farrell et al., 2021; Planavsky et al., 2023). For instance, total organic carbon (TOC), phosphorus (P), biogenic barium (Ba_{bio}), copper (Cu), zinc (Zn), nickel (Ni), etc., enable reconstructing marine primary productivity and carbon cycle perturbations, thereby revealing mechanisms driving past climate fluctuations (Scott et al., 2013; Schoepfer et al., 2015; Shen et al., 2015; Schoepfer et al., 2016; Xiang et al., 2018; Jin et al., 2020; Tribovillard, 2021; Wang et al., 2022; Zhang et al., 2022; Li et al., 2023; Sweere et al., 2023; Zhao et al., 2023). Elements such as uranium (U), vanadium (V), and molybdenum (Mo) can reveal how marine redox conditions changed during critical periods in animal evolution, including mass extinctions and evolutionary radiations (Algeo and Liu, 2020; Schobben et al., 2020; Stockey et al., 2024). Oxygen isotopes ($\delta^{18}O$) from fossilized marine organisms can reveal oceanic palaeo-temperature changes (Veizer and Prokoph, 2015; Song et al., 2019; Grossman and Joachimski, 2020; Scotese et al., 2021; Judd et al., 2022). However, many geochemical studies have focused on high-resolution research of limited time intervals and/or regions, and there is little comprehensive exploration across large-scale geological time and globally.

Fortunately, with more journals and institutions adopting strict data archiving rules and promoting adherence to FAIR (Findability, Accessibility, Interoperability, and Reusability) principles (Wilkinson et al., 2016; “FAIR Play in Geoscience Data,” 2019), a large amount of geochemical data has become accessible, and sample meta-data records are more detailed. Several geochemical databases of varying scales and foci have emerged, such as the following:

- EarthChem, which covers igneous, sedimentary, and metamorphic rocks and comprises numerous joint databases (https://www.earthchem.org/, last accessed: 16 July 2024).
- Petrological Database of the Ocean Floor (PetDB), which includes elemental chemical, isotopic, and mineralogical data of global ocean floor igneous rocks, metamorphic rocks, minerals, and inclusions (https://www.earthchem.org/petdb, last accessed: 16 July 2024).
- Geochemistry of Rocks of the Oceans and Continents (GEOROC), a comprehensive compilation

of chemical, isotopic, and other data on igneous rock samples, including whole rock, glass, mineral, and inclusion analyses and metadata (http://georoc.mpch-mainz.gwdg.de, last access: 16 July 2024).

- Data Publisher for Earth & Environmental Science (PANGAEA), which is used for archiving, publishing, and disseminating georeferenced data from earth, environmental, and biodiversity sciences and includes a large number of sediment core data (https://www.pangaea.de, last accessed: 16 July 2024).
- Stable Isotope Database for Earth System Research (StabisoDB) containing $\delta^{18}O$ and $\delta^{13}C$ data for more than 67,000 macrofossil and microfossil samples, including benthic and planktonic foraminifera, benthic and nektonic mollusks, brachiopods, fish teeth, and conodonts (https://cnidaria.nat.uni-erlangen.de/stabisodb/, last accessed: 16 July 2024).
- Sedimentary Geochemistry and Paleoenvironments Project (SGP), which collects multi-proxy sedimentary geochemical data with an emphasis on Neoproterozoic-Palaeozoic shale data in its first data release (https://sgp-search.io/, last accessed: 12 June 2024).
- NOAA and MMS Marine Minerals Geochemical Database, which contains geochemical analyses and auxiliary information on present-day marine deposits of primarily ferromanganese nodules and crusts, as well as some data for heavy minerals and phosphorites (https://www.ncei.noaa.gov/access/metadata/landing-page/bin/iso?id=gov.noaa.ngdc.mgg.geology:G01323, last accessed: 7 January 2025).
- An International Study of the Marine Biogeochemical Cycles of Trace Elements and Isotopes (GEOTRACES), which provides hydrographical and marine geochemical data acquired over the past decade (https://www.geotraces.org/, last accessed: 7 January 2025).

Many other government initiatives also host databases:

- The United States Geological Survey (USGS) National Geochemical Database, an archive of geochemical information and related metadata from USGS research (https://www.usgs.gov/energy-and-minerals/mineral-resources-program/science/national-geochemical-database, last accessed: 16 July 2024).
- The British Geological Survey (BGS), which provides data and information on UK geology, boreholes, geomagnetism, groundwater, rocks, etc. (http://www.bgs.ac.uk/, last accessed: 16 July 2024).

- The Australian National Whole Rock Geochemistry Database (OZCHEM), including chemical compositions of rock, soil, and sediment samples (https://ecat.ga.gov.au/geonetwork/srv/, last accessed: 16 July 2024).

Although some of these databases (Table 1) include data on ancient marine sediments, they have shortcomings such as limited spatial coverage, the lack of age data and coarse age resolution, the absence of recent publications, and missing information from original publications. Thus, we propose the Deep-Time Marine Sedimentary Element Database (DM-SED), which focuses on the elemental content changes in marine sediments across geological history. The current version of the DM-SED database contains 63,627 entries, enabling research on a series of scientific issues related to palaeoenvironmental, palaeoclimatic, and elemental cycles in deep-time Earth history.

DM-SED version 0.0.1 is presented in table (.csv) format. Dynamic versions of the most recent release can be found on Zenodo (https://doi.org/10.5281/zenodo.14771859, last accessed: 30 January 2025) (Lai et al., 2025), and a static copy of Version 0.0.1 is archived in the Geobiology database (http://202.114.198.132/dmgeo-geobiology-portal/, last accessed: 25 September 2024). In the following sections, we provide a brief overview of the database, information on the data sources and selection criteria, and a review of the definitions and decisions behind the metadata fields associated with each proxy measurement. We explore the spatial and temporal distribution trends of the compiled data and discuss future uses and limitations of the database.

Table 1. Overview of different databases (Note: not all databases have a clear number of records).

Database name	Content	Website information	Number of records	Data regions
EarthChem	Igneous, sedimentary, and metamorphic rocks; various joint databases	https://www.earthchem.org/, last accessed: 16 July 2024	Over 2,596 digital content files in EarthChem Library	Global
PetDB	Elemental chemical, isotopic, and mineralogical data of global ocean floor rocks	https://www.earthchem.org/petdb, last accessed: 16 July 2024	Over 6,000,000 samples	Global
GEOROC	Chemical, isotopic, and other data on igneous rock samples	http://georoc.mpch-mainz.gwdg.de, last access: 16 July 2024	672,990 samples	Global
PANGAEA	Georeferenced data from earth, environmental, and biodiversity sciences	https://www.pangaea.de, last accessed: 16 July 2024	Extensive dataset	Global
StabisoDB	$\delta^{18}O$ and $\delta^{13}C$ data for macrofossil and microfossil samples	https://cnidaria.nat.uni-erlangen.de/stabisodb/, last accessed: 16 July 2024	Over 67,000 samples	Global
SGP	Multi-proxy sedimentary geochemical data from the Palaeozoic and Neoproterozoic	https://sgp-search.io/, last accessed: 12 June 2024	82,578 samples	Global
NOAA and MMS Marine Minerals Geochemical Database	Geochemical analyses on ferromanganese nodules and crusts, as well as some heavy minerals and phosphorites	https://www.ncei.noaa.gov/access/metadata/landing-page/bin/iso?id=gov.noaa.ngdc.mgg.geology:G01323, last accessed: 7 January 2025	Over 140,000 element/oxide analyses	Global
GEOTRACES	Hydrographical and marine geochemical data	https://www.geotraces.org/, last accessed: 7 January 2025	77 cruises and more than 800 hydrographic and geochemical parameters	Global
USGS	Geochemical information and related metadata from USGS research	https://www.usgs.gov/energy-and-minerals/mineral-resources-program/science/national-geochemical-database, last accessed: 16 July 2024	Extensive dataset	United States
BGS	Data on UK geology, boreholes, geomagnetism, groundwater, rocks, etc.	http://www.bgs.ac.uk/, last accessed: 16 July 2024	Extensive dataset	United Kingdom
OZCHEM	Chemical compositions of rock, soil, and sediment samples	https://ecat.ga.gov.au/geonetwork/srv/, last accessed: 16 July 2024	Extensive dataset	Australia

2 Dataset overview

The DM-SED aims at collecting geochemical data from deep-time marine sediments. The database is primarily sourced from the SGP database, supplemented with additional 34,874 newly compiled entries. The SGP contains a total of 82,578 entries, from which we selected 28,753 entries specifically related to marine sedimentary geochemical data, and is comprised of three parts: two parts from the U.S. Geological Survey (USGS), i.e. the National Geochemical Database (USGS NGDB, https://mrdata.usgs.gov/ngdb/rock, last accessed: 9 September 2024) and the Global Geochemical Database for Critical Metals in Black Shales project (USGS CMIBS, Granitto et al., 2017), with samples mainly from North America and Phanerozoic shales from various continents, respectively (Farrell et al., 2021). The third part comprises direct inputs by SGP members. The direct inputs in the Phase 1 SGP data release primarily focused on Neoproterozoic–Palaeozoic shales, although there are other lithologies and other time periods represented (Farrell et al., 2021). Our DM-SED database, built upon the SGP, includes a new compilation of 34,874 entries from 433 studies, spanning approximately 3800 Ma and including entries from North America, Europe, Asia, Africa, South America, Oceania, Pacific and Atlantic. This supplements the temporal and spatial distribution gaps in the SGP database, thereby creating a more comprehensive sedimentary marine geochemical database. The new compiled literatures span the time range from 1965 to 2023, with the number of papers per decade gradually increasing (Fig. 1). It should be noted that the top of the DM-SED version 0.0.1 data is the new compilation, and the bottom contains data imported from SGP.

Table 2. Summary of data entries and points in the DM-SED.

	Entries	Data points
New compilation	34,874	1,454,400
SGP	28,753	1,067,855
DM-SED	63,627	2,522,255

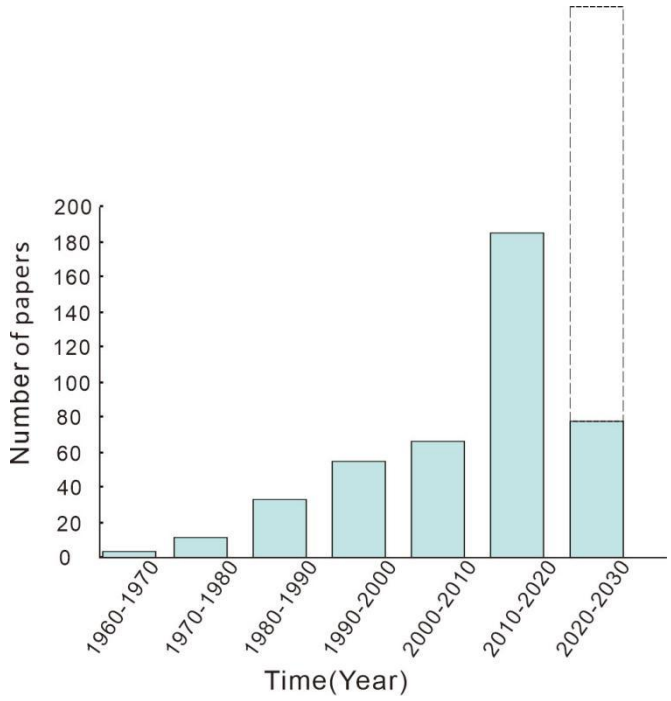

Figure 1. The distribution of publication years for newly compiled literature (the dashed line denotes the predicted literature from 2023 to 2030).

The DM-SED database comprises 63,627 entries with 2,522,255 discrete data points (Table 2), each including location (SampleID, SampleName, SiteName, Region, Elevation, SampleDepth, ModLat, ModLon, PalaeoLat, PalaeoLon), age (Age, Period, Stage, Biozone), stratigraphic information (LithName, LithType, Formation, Facies), carbon element (total carbon (Total C), inorganic carbon (C_{inorg}), TOC, in wt%), isotopic values ($\delta^{18}O_{carb}$, $\delta^{13}C_{Ker}$, $\delta^{13}C_{TOC}$, $\delta^{13}C_{carb}$, $\delta^{34}S_{CAS}$, $\delta^{34}S_{pyr}$, $\delta^{15}N_{total}$, $\delta^{15}N_{org}$, in ‰), major element (P, Al, Si, Ti, Fe, Ca, Mg, Na, K, S, N, in wt%), trace element (Ag, Ar, As, B, Ba, Be, Bi, Br, Cd, Ce, Co, Cr, Cs, Cu, Dy, Er, Eu, Ga, Gd, Ge, Hf, Hg, Ho, In, La, Li, Lu, Mn, Mo, Nb, Nd, Ni, Pb, Pr, Rb, Re, Sb, Sc, Se, Sm, Sn, Sr, Ta, Tb, Te, Th, Tl, Tm, U, V, W, Y, Yb, Zn, Zr, in ppm), methodology (TOC methods, Major elements methods, Trace elements methods), and data sources (Reference, Project). The specific names and descriptions of each field in the database are shown in Table 3. The standards and descriptions of isotope ratios in the database are shown in Table 4.

160 **Table 3. Field names and descriptions.**

Field name	Description of field (units)
Location fields	
SampleID	Unique sample identification code
SampleName	Author denoted title for the sample (often non-unique)
SiteName	Name of the drill core site or section
Region	Country or ocean of the data collection site
Elevation	Distance between sampling location and sea level (m)
SampleDepth	Stratigraphic height or depth (m)
ModLat	Modern latitude of collection site rounded to two decimals; negative values indicate the Southern Hemisphere (decimal degrees)
ModLon	Modern longitude of the collection site rounded to two decimals; negative values indicate the Western Hemisphere (decimal degrees)
PalaeoLat	Palaeolatitude of collection site rounded to two decimals; negative values indicate the Southern Hemisphere (decimal degrees)
PalaeoLon	Palaeolongitude of the collection site rounded to two decimals; negative values indicate the Western Hemisphere (decimal degrees)
Age fields	
Age	Absolute Age, in reference to GTS2020 (Ma)
Period	The geologic period
Stage	The geologic stage (i.e. geochronologic age)
Biozone	Conodont, graptolite, ammonite biozone, etc
Stratigraphy	
LithName	Lithological name of the sample, as originally published
LithType	Lithology type of sample (e.g. carbonate, siliciclastic)
Formation	Geologic formation name
Facies	Depositional environment (e.g. mid-shelf, ramp)
Proxy fields	
Carbon	The content of carbon, including Total C, C_{inorg}, TOC, rounded to two decimals (wt%)
Isotopes	The isotope value, rounded to two decimals (‰)
Major elements	The content of major elements such as P, Al, and Si, rounded to two decimals (wt%)
Trace elements	The content of trace elements such as Ag, Ar, As, B, and Ba, rounded to two decimals (ppm)
Methodology	
TOC methods	A brief description of the testing methods for TOC
Major elements methods	A brief description of the testing methods for major elements
Trace elements methods	A brief description of the testing methods for trace elements
Data sources	
Reference	Data sources, including published literature or other databases
Project	Two parts: new compilation and SGP

161

Table 4. Standards and descriptions of isotope ratios in the DM-SED.

Symbol	Standard	Description
$\delta^{18}O_{carb}$	Vienna Pee Dee Belemnite (VPDB)	Oxygen isotope ratio of carbonate minerals, used in palaeoclimate studies.
$\delta^{13}C_{Ker}$	VPDB	Carbon isotope ratio of kerogen, used to study the source and depositional environment of organic matter.
$\delta^{13}C_{TOC}$	VPDB	Carbon isotope ratio of total organic carbon, used to analyse the source of organic matter and biogeochemical cycles in sediments.
$\delta^{13}C_{carb}$	VPDB	Carbon isotope ratio of carbonate minerals, used in palaeoclimate and carbon cycle research.
$\delta^{34}S_{CAS}$	Vienna Canyon Diablo Troilite (VCDT)	Sulfur isotope ratio of carbonate-associated sulfate, used to study the sulfur cycle and redox conditions.
$\delta^{34}S_{pyr}$	VCDT	Sulfur isotope ratio of pyrite, typically used to investigate the sulfur cycle and redox conditions in ancient oceans.
$\delta^{15}N_{total}$	Atmospheric Nitrogen (air N_2)	Nitrogen isotope ratio of total nitrogen, used to study the nitrogen cycle and nutrient sources.
$\delta^{15}N_{org}$	air N_2	Nitrogen isotope ratio of organic nitrogen, often used to analyse the source of organic matter and the nitrogen cycle.

3 Dataset screening and processing

This section details the screening and processing criteria for sample location, age, lithology and facies, specific geochemical values, and data source information (Fig. 2).

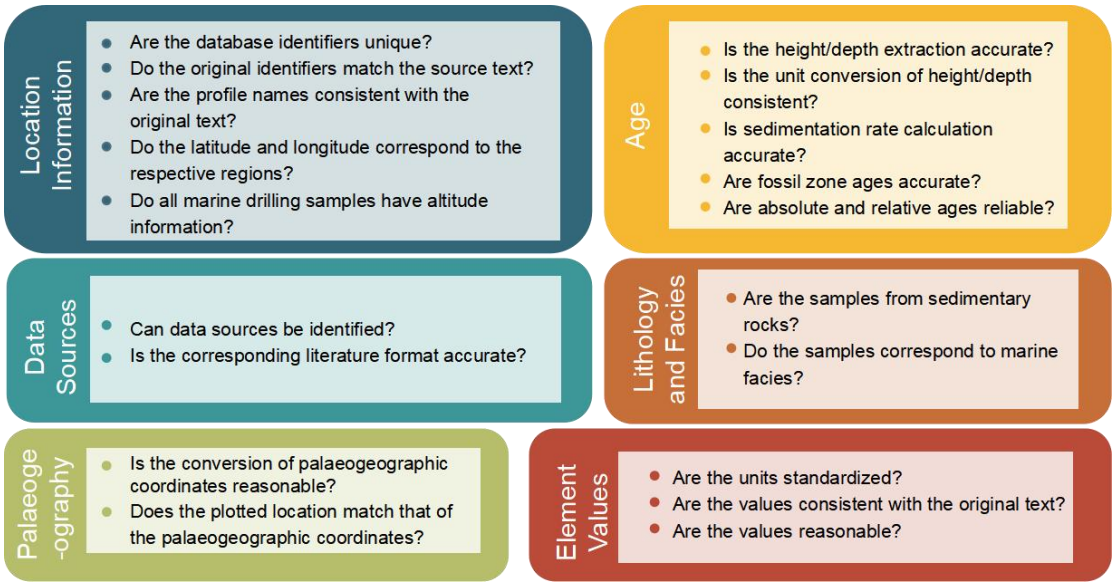

Figure 2. The data filtering and processing criteria for DM-SED.

For sample location, the database includes SampleID, SampleName, SiteName, Region, Elevation, SampleDepth, ModLat, ModLon, PalaeoLat, and PalaeoLon. A unique SampleID is assigned to each sample in the DM-SED. The SampleName corresponds to the identifier given in each referenced publication, facilitating cross-referencing with the original data. The SiteName includes well name or outcrop information, representing the smallest unit of location information. The Region indicates the country or ocean area where the sample has been collected and represents a broader geographical range. The Elevation data are mainly related to samples from the Deep Sea Drilling Project (DSDP) and the Ocean Drilling Program (ODP) collected from post-Cretaceous sediments and indicate whether the samples originate from deep or shallow marine environments. SampleDepth refers to the relative position (in metres) of the sample within the well or outcrop, which is crucial for calculating sample age. In some publications, specific heights are not provided directly but are given as relative heights through figures. We manually extracted these heights using WebPlotDigitizer, rounding to two decimal places (Drevon et al., 2017). For publications in which heights are expressed in feet or centimetres, we converted the units to metres. Modern latitude and longitude (ModLat and ModLon) information are the most precise location data. Although some publications provide exact coordinates, many offer only section names (i.e. SiteName) and regions or merely a map marking the location of the section. For publications providing section names, we determined accurate coordinates by consulting other studies carried out in the same section. For those providing only a map marking the location of the section, we used Google Maps to estimate relative coordinates. To ensure consistency, we recorded sample

coordinates in decimal degrees, rounded to two decimal places, with positive values indicating north latitude and east longitude and negative values indicating south latitude and west longitude. The coordinate reference system is WGS 84 (World Geodetic System 1984). For palaeo-coordinates, we reconstructed palaeo-latitude and palaeo-longitude (PalaeoLat, and PalaeoLon) using the sample age and modern coordinates, employing the PointTracker v7 rotation files from the PALEOMAP project, which are based on current geographic reference data and global tectonic history models (Scotese, 2008). It is important to note that we only generated palaeogeographic locations for samples from the Phanerozoic, as the geological records from this time are more complete and abundant compared to those from the Precambrian, making the reconstruction of geographic features (such as ancient oceans, mountains, plains, etc.) relatively more reliable and accurate (Scotese and Wright 2018). We plotted the sample points on palaeogeographic maps based on Scotese's data using QGIS 3.16 (Scotese and Wright 2018).

To assign specific ages to each sample in the database, we assumed a constant sedimentation rate within the same formation or group of section. If the original studies provided numerical ages for two or more samples, we calculated the precise age for each sample based on the sedimentation rate and assigned it accordingly. If absolute ages were not provided in the original literature, we assigned approximate ages based on corresponding fossil zones or the general age of the same lithostratigraphic unit in the same region (Farrell et al., 2021; Judd et al., 2022). For samples with completely missing height information in the original text, we assigned the same age to all samples within the section based on lithostratigraphic information. However, the primary age constraints for these samples (mainly from USGS NGDB and USGS CMIBS) remain derived from SGP age calls. Once each sample had a specific age, we assigned it to a specific Period and Stage according to its age. We attempted to incorporate the most recent age models; however, due to the extensive size of the data compilation, it was not feasible to update all of them. All ages were based on the timescale provided by the Geologic Time Scale 2020 (Gradstein et al., 2020). Although GTS 2020 is accurate, readers are advised to consult the incremental updates of the International Chronostratigraphic Chart (ICS) for the most accurate stratigraphic intervals.

For lithology and facies, the lithologies include shale, mudstone, sandstone, limestone, dolostone, and others. We classified these into two types of rocks: siliciclastic sedimentary rocks (88.7%) and carbonate rocks (11.3%). For outcrop sections, the lithostratigraphic unit was generally available;

however, for data from marine drilling sites, there was often no corresponding lithostratigraphic unit information. Regarding facies classification, before the Cretaceous, the primary depositional environment was marine settings on continental crust, including specific facies such as inner shelves, outer shelves, and basinal. However, after the Cretaceous, with most samples coming from the DSDP and ODP, shallow marine depositional environments still existed and were sampled, but deep-sea pelagic settings began to be sampled as well.

For specific geochemical values in the DM-SED database, we standardized the units, converting oxides to elements (e.g. P (ppm) to P (wt%), P_2O_5 (wt%) to P (wt%)). If a sample was analysed multiple times, we averaged the value. For literature before 2000, some data were preserved as images, requiring manual extraction of values, and some images were slightly blurry, potentially leading to minor human error. We excluded data that were beyond detection limits (e.g. the trace element content is too low and the value provided in the text represents the minimum detection limit) or unreasonable (e.g. negative values for major and trace elements).

For the geochemical methodology, we briefly documented them based on the descriptions in the original text, focusing primarily on the testing methods and instrument models used for TOC, major elements, and trace elements. Methods for stable isotopes were not documented, as the testing methods vary for different isotopes, and due to the limited amount of isotope data, recording them holds little significance.

Regarding data sources, we ensured that each corresponding reference was collected and listed in full citation format, including authors, title, publication date, journal, page numbers, and DOI. Most data in the SGP database came directly from USGS NGDB and USGS CMIBS, without corresponding literature sources, so we marked them individually. The entire database for this Project was divided into two parts: new compilation and SGP. We used keyword searches in Google Scholar to identify missing references and made efforts to target literature for data-scarce regions (e.g. South America) and time intervals (e.g. Silurian, Jurassic).

4 Data distribution

The elemental data content distribution for the entire database is shown in Fig. 3. Overall, major elements have the highest data quantity, followed by trace elements and carbon elements, with isotope

data having the lowest quantity. Among the major elements, N has the fewest entries, with 3,164 records, whereas the other major elements all have more than 10,000 entries. Al has the highest quantity, with 51,906 records. Among trace elements, Mn has the largest record (42,499 records), followed by Ba (41,471 records). Ar and Br have the fewest records, with 9 and 176 records, respectively. Other elements such as Ag, B, Bi, Ge, Hg, In, Re, Se, Sn, Te, Tl, Tm, and W have data quantities ranging from 1,000 to 10,000. Elements such as As, Be, Cd, Ce, Co, Cr, Cs, Cu, Dy, Er, Eu, Ga, Gd, Hf, Ho, La, Li, Lu, Mo, Nb, Nd, Ni, Pb, Pr, Rb, Sb, Sc, Sm, Sr, Ta, Tb, Th, U, V, Y, Yb, Zn, and Zr all have more than 10,000 records each. For carbon elements, TOC has the largest record (32,906 entries), followed by Total C (9,386 entries), while C_{inorg} has the lowest record (7,215 entries). Isotope data are overall less abundant, with none exceeding 10,000 entries; the most abundant is $\delta^{13}C_{TOC}$, with 8,166 records, and the least abundant is $\delta^{13}C_{Ker}$, with only 112 records.

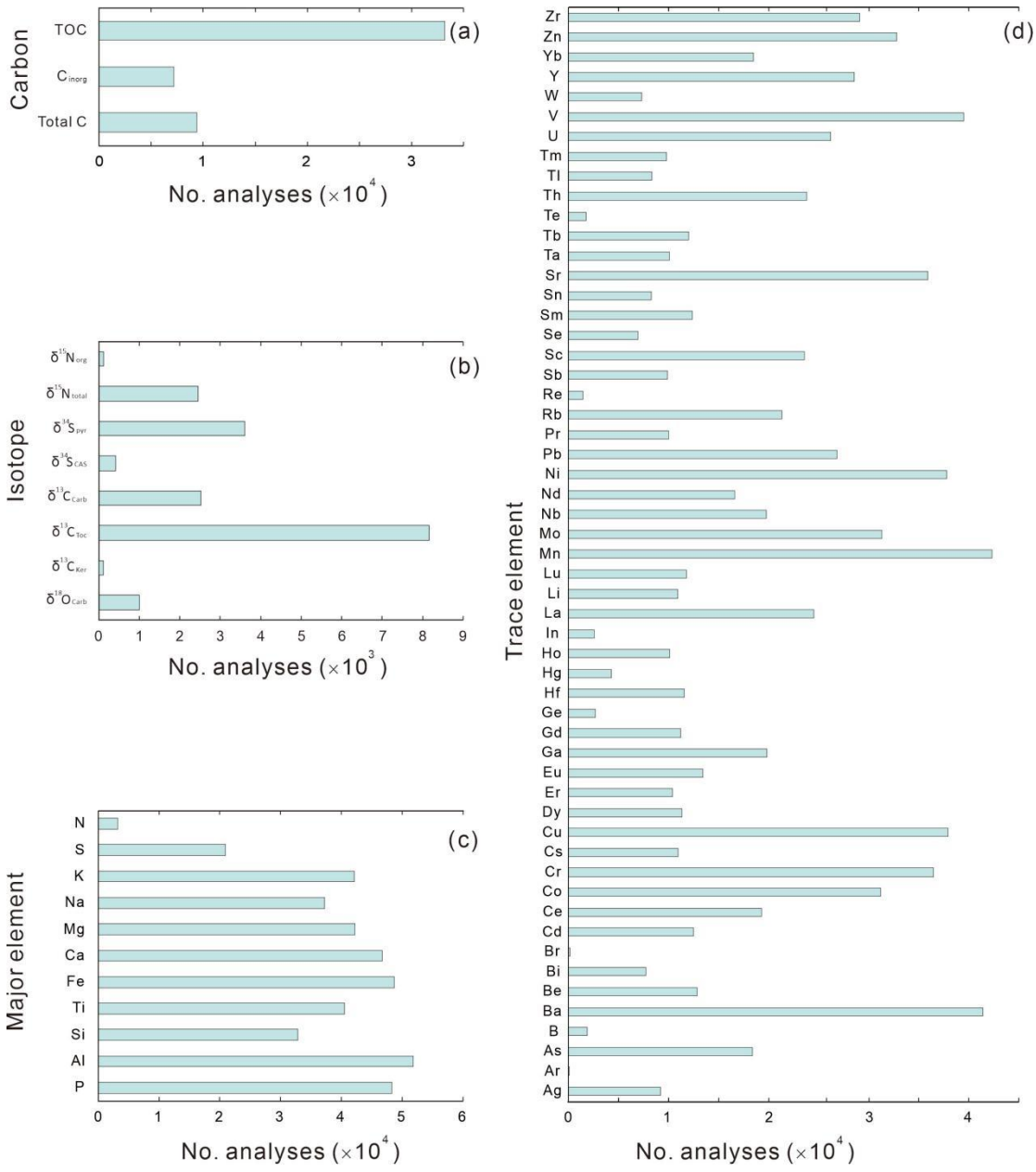

Figure 3. Histogram distribution of different subsets. (a) Carbon elements. (b) Isotopes. (c) Major elements. (d) Trace elements.

The temporal trend of data density in the entire database, shown in Fig. 4a, indicates that the data are primarily distributed in the Phanerozoic Eon, which accounts for 85% of the entire database. Within the Phanerozoic, the Cenozoic Era accounts for 19% of the database, the Mesozoic Era accounts for 21%, and the Palaeozoic Era accounts for 45%. Precambrian data account for only 15% of the entire database. The SGP data are most concentrated in the Palaeozoic Era, in which they make up 27% of the total database, with the new compiled data contributing only 18%. In other eras, the new compiled data outnumber the SGP data: 4% versus 15% in the Cenozoic, 7% versus 14% in the Mesozoic, and 7%

versus 8% in the Precambrian. This is mainly the case because the SGP data in the first phase were primarily from the Neoproterozoic and Palaeozoic eras (Farrell et al., 2021).

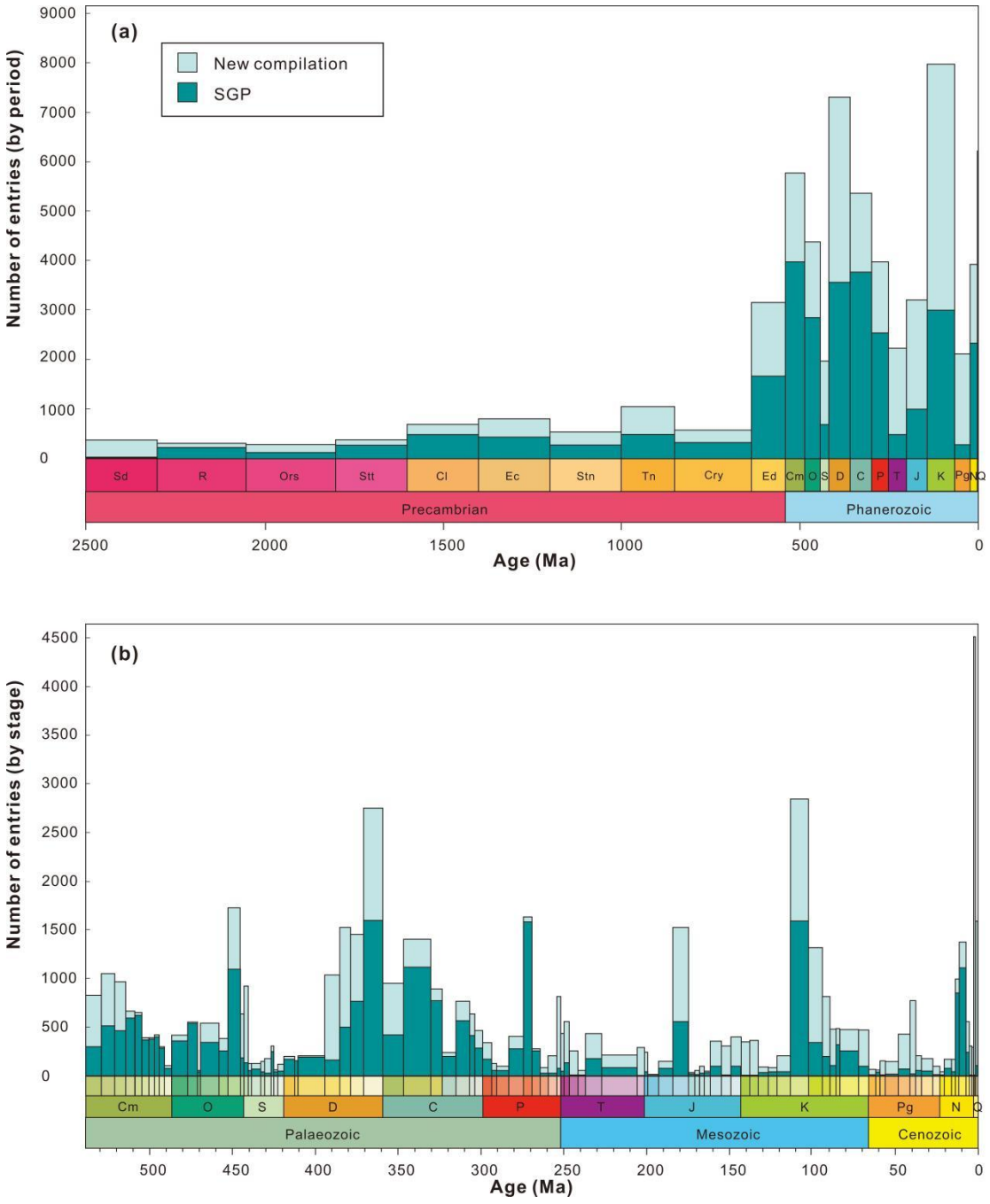

Figure 4. The age distribution of samples in the database. (a) Age distribution of samples (excluding a small number of samples with ages >2500 Ma from the figure, a total of 1258 samples). (b) Age distribution of Phanerozoic samples at the stage level. Sd, Siderian; R, Rhyacian; Sd, Siderian; Ors, Orosirian; Stt, Statherian; Cl, Calymmian; Ec, Ectasian; Stn, Stenian; Tn, Tonian; Cry, Cryogenian; Ed, Ediacaran; Cm, Cambrian; O, Ordovician; S, Silurian; D, Devonian; C, Carboniferous; P, Permian; T, Triassic; J, Jurassic; K, Cretaceous; Pg, Paleogene; N, Neogene; Q, Quaternary.

For the distribution of sample ages within the Phanerozoic, we divided the samples by stage, as shown in Fig. 4b. For the Quaternary Period, due to its short duration, the data were not subdivided by Stage but were instead divided into the Holocene and Pleistocene Series. Data distribution is not uniform, with the highest concentration in the Quaternary Period. These data mainly come from DSDP and ODP, which are characterised by a high number of core samples and high resolution. There are fewer data for the Upper Permian, Lower Triassic, and Lower to Middle Jurassic, possibly because of the existence of Pangaea at that time, which reduced the area of continental margins and inhibited marine transgressions, resulting in fewer preserved marine environments in comparison to those of other geological periods (Mackenzie and Pigott, 1981; Walker et al., 2002). The distribution of sample quantities in other periods fluctuates, often corresponding to periods of significant research interest, such as the end-Ordovician, end-Devonian, end-Permian, Early Jurassic Toarcian and Early Cretaceous Albian, which had peaks in sample numbers due to their association with major mass extinction events and oceanic anoxic events (Fan et al., 2020).

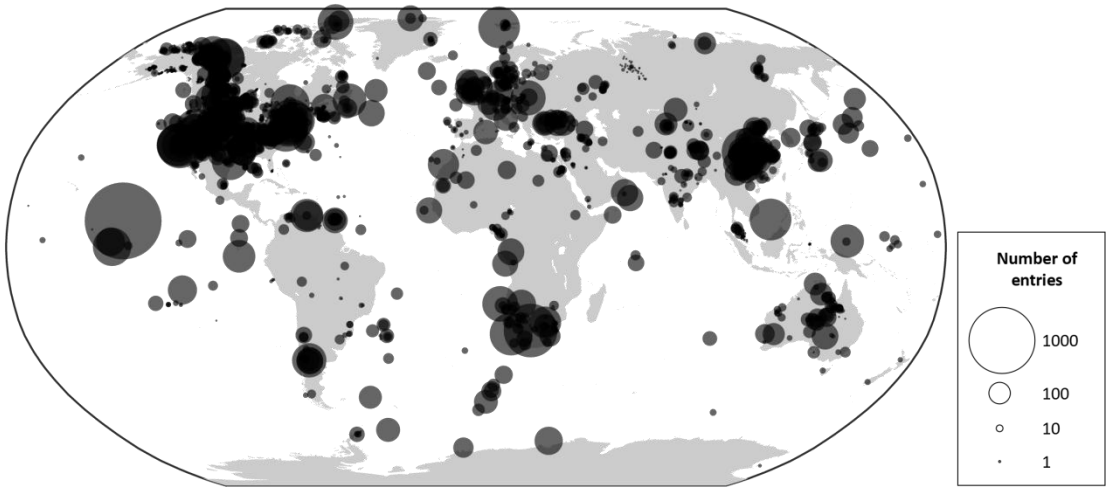

Figure 5. Bubble chart of modern geographical distribution and sample quantities in the database.

In terms of spatial trends, the spatial distribution of sampling points in the DM-SED database is inherently uneven, both in modern and palaeogeographic locations. Modern locations are primarily concentrated in North America, Europe, South Africa, and China (Fig. 5). When modern coordinates are converted to palaeogeographic coordinates and projected onto palaeogeographic maps, Cambrian to Jurassic data come predominantly from continental margin environments, as subduction of oceanic crust before the Cretaceous resulted in preservation of very few deep-sea environments (Fig. 6). Cambrian and Ordovician data are distributed mainly on the Laurentia, Baltica, and South China plates,

with a few along the Gondwana margin. Silurian data occur mainly on Laurentia, South China, and eastern Gondwana. Devonian and Carboniferous data are primarily on the Laurussia plate, with sparse distribution in South China and Gondwana. Permian and Triassic data are mainly on the Laurussia and South China plates, with sparse distribution in Gondwana. Jurassic data are primarily on the North American, European, with sparse distribution on other plates. From the Cretaceous to the Quaternary, sample locations, dominated by data from the DSDP, ODP, and USGS NGDB projects, are mainly located in the deep oceans and North America.

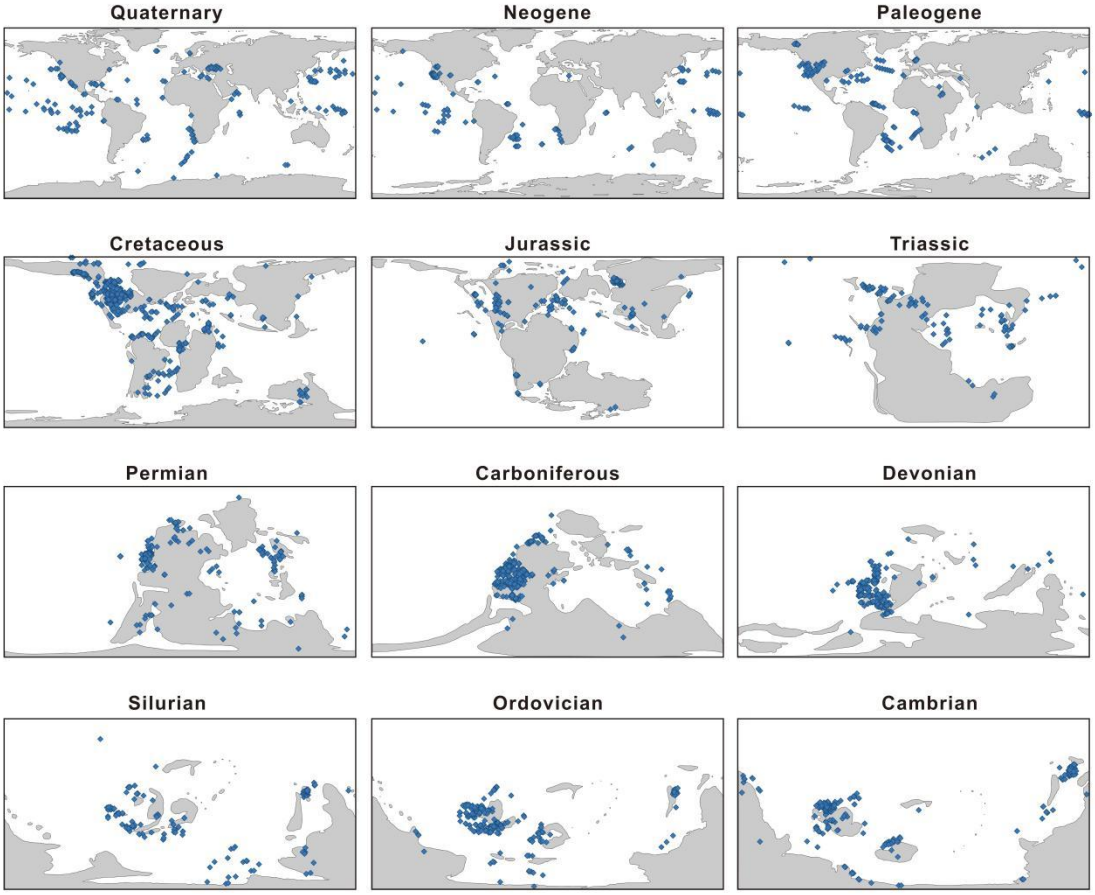

Figure 6. The palaeogeographic distribution of sample sites in the DM-SED.

When averaging all Phanerozoic data by stage and spatially averaging them into 15° palaeolatitude bins (Fig. 7), Palaeozoic data records are mainly biased toward tropical regions. Cambrian data are concentrated between 15° S and 30° N, Ordovician to Carboniferous data are concentrated between 45° S and 15° N, and Permian data are concentrated between 0° N and 30° N, with data mainly fluctuating around the equator. As continents migrated northward through the Mesozoic and into the Cenozoic, records began to show bias toward mid-latitudes in the Northern Hemisphere. From the Triassic to the Cretaceous, data are mainly concentrated between 0° N and 60°

N. Paleogene to Quaternary data are concentrated between 45° S and 45° N.

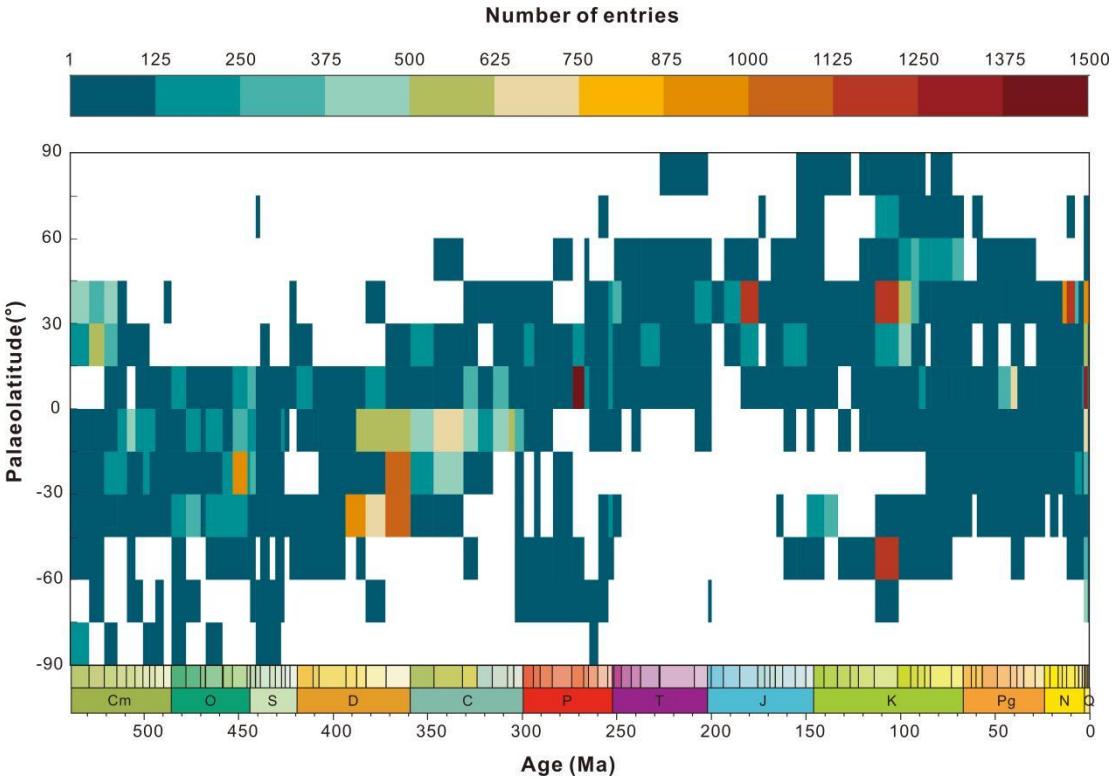

Figure 7. The spatiotemporal distributions of sample quantities (categorized temporally by stage and spatially by palaeolatitude intervals of 15°).

5 Usage instructions

The ultimate goal of the DM-SED database is to provide the geoscience community with a valuable resource of knowledge and geographic information. By deriving meaningful conclusions from a large marine sediment geochemistry database, we aim to enhance our understanding of Earth's environmental changes over time and space. All entries in DM-SED contain the source of original proxy values, ensuring traceability between DM-SED and the original datasets from which the data were extracted.

However, our database has some limitations. The criteria for age determination, relying variously on fossil zones and lithostratigraphic unit information, are not entirely uniform. Some age determinations are still coarse, with samples from a single section all assigned the same age. Additionally, the data quantity for some elements is still low. There may be significant differences in methodological precision between older and newer literature. Currently, these issues remain largely unresolved. Despite our best efforts to identify data from the literature and process quality control for

each entry, the sheer volume of data in DM-SED means that some errors or omissions are inevitable. Prompt corrections and continuous updates are expected to ensure the credibility of this database.

Finally, it is important to recognize that DM-SED merely compiles these various datasets and cannot impose any requirements on their generation. When using the data (and where practicable), we recommend citing both DM-SED and the original data sources to ensure proper attribution.

6 Data availability

Version controlled releases of the DM-SED can be found on Zenodo (https://doi.org/10.5281/zenodo.14771859, last accessed: 30 January 2025) (Lai et al., 2025). A static copy of DM-SED version 0.0.1 is archived in the Geobiology database (http://202.114.198.132/dmgeo-geobiology-portal/, last accessed: 25 September 2024). We plan to supplement and improve the database continuously and hope to collaborate with existing compilation authors to assist in adding new content.

7 Code availability

The software tools used in this study are available at the following links: WebPlotDigitizer can be downloaded from https://github.com/automeris-io/WebPlotDigitizer/releases (last accessed: 20 July 2024); the PointTracker v7 tool can be found at http://www.paleogis.com (last accessed: 20 July 2024); QGIS 3.16 can be downloaded from the https://qgis.org/project/overview/ (last accessed: 20 July 2024).

Author contributions. Jiankang Lai: Writing – original draft, Visualization, Data collection, Investigation. Haijun Song: Writing – review & editing, Supervision, Investigation, Funding acquisition. Daoliang Chu: Writing – review & editing, Investigation. Jacopo Dal Corso: Writing – review & editing, Investigation. Erik A. Sperling: Writing – review & editing, Investigation. Yuyang Wu: Writing – review & editing, Supervision, Investigation, Data collection. Xiaokang Liu: Writing – review & editing, Investigation. Lai Wei: Writing – review & editing, Data collection, Investigation.

Mingtao Li: Writing– review & editing, Investigation. Hanchen Song: Writing– review & editing, Investigation. Yong Du: Writing– review & editing, Investigation. Enhao Jia: Writing– review & editing, Investigation. Yan Feng: Writing– review & editing, Investigation. Huyue Song: Writing– review & editing, Investigation. Wenchao Yu: Writing– review & editing, Investigation. Qingzhong Liang: Writing – review & editing, Investigation. Xinchuan Li: Writing – review & editing, Investigation. Hong Yao: Writing– review & editing, Investigation.

Competing interests. The authors declare that they have no conflicts of interest.

Acknowledgements.

This paper benefited greatly from comments from Thierry Adatte and an anonymous reviewer. We also thank Jan Peter (Research Scientist, Geological Survey of Canada) for providing his literature data.

Funding:

This study was supported by the National Natural Science Foundation of China grant 42325202, the State Key R&D Project of China (2023YFF0804000), 111 Project grant B08030, Natural Science Foundation of Hubei (2023AFA006), and Graduate Student Project from the Hubei Research Center for Basic Disciplines of Earth Sciences (NO. HRCES-202413). E.A.S. is supported by United States National Science Foundation grant EAR-2143164.

REFERENCES

Algeo, T. J. and Liu, J.: A re-assessment of elemental proxies for paleoredox analysis, Chem. Geol., 540, 119549, https://doi.org/10.1016/j.chemgeo.2020.119549, 2020.

Drevon, D., Fursa, S. R., and Malcolm, A. L.: Intercoder Reliability and Validity of WebPlotDigitizer in Extracting Graphed Data, Behav. Modif., 41, 323-339, https://doi.org/10.1177/0145445516673998, 2017.

FAIR: FAIR Play in geoscience data, Nat. Geosci., 12, 961, https://doi.org/10.1038/s41561-019-0506-4, 2019.

Fan, J., Shen, S., Erwin, D. H., Sadler, P. M., MacLeod, N., Cheng, Q., Hou, X., Yang, J., Wang, X.,

Wang, Y., Zhang, H., Chen, X., Li, G., Zhang, Y., Shi, Y., Yuan, D., Chen, Q., Zhang, L., Li, C., and Zhao, Y.: A high-resolution summary of Cambrian to Early Triassic marine invertebrate biodiversity, Science, 367, 272-277, https://doi.org/10.1126/science.aax4953, 2020.

Farrell, U. C., Samawi, R., Anjanappa, S., Klykov, R., Adeboye, O. O., Agic, H., Ahm, A. C., Boag, T. H., Bowyer, F., Brocks, J. J., Brunoir, T. N., Canfield, D. E., Chen, X., Cheng, M., Clarkson, M. O., Cole, D. B., Cordie, D. R., Crockford, P. W., Cui, H., Dahl, T. W., Mouro, L. D., Dewing, K., Dornbos, S. Q., Drabon, N., Dumoulin, J. A., Emmings, J. F., Endriga, C. R., Fraser, T. A., Gaines, R. R., Gaschnig, R. M., Gibson, T. M., Gilleaudeau, G. J., Gill, B. C., Goldberg, K., Guilbaud, R., Halverson, G. P., Hammarlund, E. U., Hantsoo, K. G., Henderson, M. A., Hodgskiss, M. S. W., Horner, T. J., Husson, J. M., Johnson, B., Kabanov, P., Brenhin Keller, C., Kimmig, J., Kipp, M. A., Knoll, A. H., Kreitsmann, T., Kunzmann, M., Kurzweil, F., LeRoy, M. A., Li, C., Lipp, A. G., Loydell, D. K., Lu, X., Macdonald, F. A., Magnall, J. M., Mand, K., Mehra, A., Melchin, M. J., Miller, A. J., Mills, N. T., Mwinde, C. N., O'Connell, B., Och, L. M., Ossa Ossa, F., Pages, A., Paiste, K., Partin, C. A., Peters, S. E., Petrov, P., Playter, T. L., Plaza-Torres, S., Porter, S. M., Poulton, S. W., Pruss, S. B., Richoz, S., Ritzer, S. R., Rooney, A. D., Sahoo, S. K., Schoepfer, S. D., Sclafani, J. A., Shen, Y., Shorttle, O., Slotznick, S. P., Smith, E. F., Spinks, S., Stockey, R. G., Strauss, J. V., Stueken, E. E., Tecklenburg, S., Thomson, D., Tosca, N. J., Uhlein, G. J., Vizcaino, M. N., Wang, H., White, T., Wilby, P. R., Woltz, C. R., Wood, R. A., Xiang, L., Yurchenko, I. A., Zhang, T., Planavsky, N. J., Lau, K. V., Johnston, D. T., and Sperling, E. A.: The Sedimentary Geochemistry and Paleoenvironments Project, Geobiology, 19, 545-556, https://doi.org/10.1111/gbi.12462, 2021.

Gradstein, F. M., Ogg, J. G., Schmitz, M. D., and Ogg, G. M.: Geologic time scale 2020, Elsevier, 2020.

Granitto, M., Giles, S. A., and Kelley, K. D.: Global Geochemical Database for Critical Metals in Black Shales, U.S. Geological Survey data release [data set], https://doi.org/10.5066/F71G0K7X, 2017.

Grossman, E. L. and Joachimski, M. M.: Oxygen Isotope Stratigraphy, in: Geologic Time Scale 2020, 279-307, https://doi.org/10.1016/b978-0-12-824360-2.00010-3, 2020.

Jin, C., Li, C., Algeo, T. J., Wu, S., Cheng, M., Zhang, Z., and Shi, W.: Controls on organic matter accumulation on the early-Cambrian western Yangtze Platform, South China, Mar. Pet. Geol.,

111, 75-87, https://doi.org/10.1016/j.marpetgeo.2019.08.005, 2020.

Judd, E. J., Tierney, J. E., Huber, B. T., Wing, S. L., Lunt, D. J., Ford, H. L., Inglis, G. N., McClymont, E. L., O'Brien, C. L., Rattanasriampaipong, R., Si, W., Staitis, M. L., Thirumalai, K., Anagnostou, E., Cramwinckel, M. J., Dawson, R. R., Evans, D., Gray, W. R., Grossman, E. L., Henehan, M. J., Hupp, B. N., MacLeod, K. G., O'Connor, L. K., Sanchez Montes, M. L., Song, H., and Zhang, Y. G.: The PhanSST global database of Phanerozoic sea surface temperature proxy data, Sci. Data, 9, 753, https://doi.org/10.1038/s41597-022-01826-0, 2022.

Lai, J., Song, H., Chu, D., Dal Corso, J., Sperling, E. A., Wu, Y., Liu, X., Wei, L., Li, M., Song, H., Du, Y., Jia, E., Feng, Y., Song, H., Yu, W., Liang, Q., Li, X., and Yao, H.: Deep-Time Marine Sedimentary Element Database [data set], Zenodo. https://doi.org/10.5281/zenodo.14771859, 2025.

Large, R. R., Halpin, J. A., Lounejeva, E., Danyushevsky, L. V., Maslennikov, V. V., Gregory, D., Sack, P. J., Haines, P. W., Long, J. A., Makoundi, C., and Stepanov, A. S.: Cycles of nutrient trace elements in the Phanerozoic ocean, Gondwana Res., 28, 1282-1293, https://doi.org/10.1016/j.gr.2015.06.004, 2015.

Li, Z., Zhang, Y. G., Torres, M., and Mills, B. J. W.: Neogene burial of organic carbon in the global ocean, Nature, 613, 90-95, https://doi.org/10.1038/s41586-022-05413-6, 2023.

Mackenzie, F. T. and Pigott, J. D.: Tectonic controls of Phanerozoic sedimentary rock cycling, J. Geol. Soc., 138, 183-196, https://doi.org/10.1144/gsjgs.138.2.0183, 1981.

Planavsky, N. J., Asael, D., Rooney, A. D., Robbins, L. J., Gill, B. C., Dehler, C. M., Cole, D. B., Porter, S. M., Love, G. D., Konhauser, K. O., and Reinhard, C. T.: A sedimentary record of the evolution of the global marine phosphorus cycle, Geobiology, 21, 168-174, https://doi.org/10.1111/gbi.12536, 2023.

Reinhard, C. T., Planavsky, N. J., Gill, B. C., Ozaki, K., Robbins, L. J., Lyons, T. W., Fischer, W. W., Wang, C., Cole, D. B., and Konhauser, K. O.: Evolution of the global phosphorus cycle, Nature, 541, 386-389, https://doi.org/10.1038/nature20772, 2017.

Schobben, M., Foster, W. J., Sleveland, A. R. N., Zuchuat, V., Svensen, H. H., Planke, S., Bond, D. P. G., Marcelis, F., Newton, R. J., Wignall, P. B., and Poulton, S. W.: A nutrient control on marine anoxia during the end-Permian mass extinction, Nat. Geosci., 13, 640-646, https://doi.org/10.1038/s41561-020-0622-1, 2020.

Schoepfer, S. D., Algeo, T. J., Ward, P. D., Williford, K. H., and Haggart, J. W.: Testing the limits in a greenhouse ocean: Did low nitrogen availability limit marine productivity during the end-Triassic mass extinction?, Earth Planet. Sci. Lett., 451, 138-148, https://doi.org/10.1016/j.epsl.2016.06.050, 2016.

Schoepfer, S. D., Shen, J., Wei, H., Tyson, R. V., Ingall, E., and Algeo, T. J.: Total organic carbon, organic phosphorus, and biogenic barium fluxes as proxies for paleomarine productivity, Earth Sci. Rev., 149, 23-52, https://doi.org/10.1016/j.earscirev.2014.08.017, 2015.

Scotese, C.: The PALEOMAP Project PaleoAtlas for ArcGIS, version 1, 2, 16-31, 2008.

Scotese, C. R., Song, H., Mills, B. J. W., and van der Meer, D. G.: Phanerozoic paleotemperatures: The earth's changing climate during the last 540 million years, Earth Sci. Rev., 215, 103503, https://doi.org/10.1016/j.earscirev.2021.103503, 2021.

Scotese, C. R. and Wright, N.: PALEOMAP Paleodigital Elevation Models (PaleoDEMS) for the Phanerozoic PALEOMAP Project, Paleomap Proj, https://www.earthbyte.org/paleodem-resourcescotese-and-wright-2018/, 2018.

Scott, C., Planavsky, N. J., Dupont, C. L., Kendall, B., Gill, B. C., Robbins, L. J., Husband, K. F., Arnold, G. L., Wing, B. A., Poulton, S. W., Bekker, A., Anbar, A. D., Konhauser, K. O., and Lyons, T. W.: Bioavailability of zinc in marine systems through time, Nat. Geosci., 6, 125-128, https://doi.org/10.1038/ngeo1679, 2012.

Shen, J., Schoepfer, S. D., Feng, Q., Zhou, L., Yu, J., Song, H., Wei, H., and Algeo, T. J.: Marine productivity changes during the end-Permian crisis and Early Triassic recovery, Earth Sci. Rev., 149, 136-162, https://doi.org/10.1016/j.earscirev.2014.11.002, 2015.

Song, H., Wignall, P. B., Song, H., Dai, X., and Chu, D.: Seawater Temperature and Dissolved Oxygen over the Past 500 Million Years, J. Earth Sci., 30, 236-243, https://doi.org/10.1007/s12583-018-1002-2, 2019.

Stockey, R. G., Cole, D. B., Farrell, U. C., Agić, H., Boag, T. H., Brocks, J. J., Canfield, D. E., Cheng, M., Crockford, P. W., Cui, H., Dahl, T. W., Del Mouro, L., Dewing, K., Dornbos, S. Q., Emmings, J. F., Gaines, R. R., Gibson, T. M., Gill, B. C., Gilleaudeau, G. J., Goldberg, K., Guilbaud, R., Halverson, G., Hammarlund, E. U., Hantsoo, K., Henderson, M. A., Henderson, C. M., Hodgskiss, M. S. W., Jarrett, A. J. M., Johnston, D. T., Kabanov, P., Kimmig, J., Knoll, A. H., Kunzmann, M., LeRoy, M. A., Li, C., Loydell, D. K., Macdonald, F. A., Magnall, J. M., Mills, N. T., Och, L. M.,

O'Connell, B., Pagès, A., Peters, S. E., Porter, S. M., Poulton, S. W., Ritzer, S. R., Rooney, A. D., Schoepfer, S., Smith, E. F., Strauss, J. V., Uhlein, G. J., White, T., Wood, R. A., Woltz, C. R., Yurchenko, I., Planavsky, N. J., and Sperling, E. A.: Sustained increases in atmospheric oxygen and marine productivity in the Neoproterozoic and Palaeozoic eras, Nat. Geosci., 17, 667-674, https://doi.org/10.1038/s41561-024-01479-1, 2024.

Sweere, T. C., Dickson, A. J., and Vance, D.: Nickel and zinc micronutrient availability in Phanerozoic oceans, Geobiology, 21, 310-322, https://doi.org/10.1111/gbi.12541, 2023.

Tribovillard, N.: Re-assessing copper and nickel enrichments as paleo-productivity proxies, BSGF - Earth Sciences Bulletin, 192, 54, https://doi.org/10.1051/bsgf/2021047, 2021.

Veizer, J. and Prokoph, A.: Temperatures and oxygen isotopic composition of Phanerozoic oceans, Earth Sci. Rev., 146, 92-104, https://doi.org/10.1016/j.earscirev.2015.03.008, 2015.

Walker, L. J., Wilkinson, B. H., and Ivany, L. C.: Continental drift and Phanerozoic carbonate accumulation in shallow-shelf and deep-marine settings, J. Geol., 110, 75-87, https://doi.org/10.1086/324318, 2002.

Wang, D., Liu, Y., Zhang, J., Lang, Y., Li, Z., Tong, Z., Xu, L., Su, Z., and Niu, J.: Controls on marine primary productivity variation and organic matter accumulation during the Late Ordovician — Early Silurian transition, Mar. Pet. Geol., 142, 105742, https://doi.org/10.1016/j.marpetgeo.2022.105742, 2022.

Wilkinson, M. D., Dumontier, M., Aalbersberg, I. J., Appleton, G., Axton, M., Baak, A., Blomberg, N., Boiten, J. W., da Silva Santos, L. B., Bourne, P. E., Bouwman, J., Brookes, A. J., Clark, T., Crosas, M., Dillo, I., Dumon, O., Edmunds, S., Evelo, C. T., Finkers, R., Gonzalez-Beltran, A., Gray, A. J., Groth, P., Goble, C., Grethe, J. S., Heringa, J., t Hoen, P. A., Hooft, R., Kuhn, T., Kok, R., Kok, J., Lusher, S. J., Martone, M. E., Mons, A., Packer, A. L., Persson, B., Rocca-Serra, P., Roos, M., van Schaik, R., Sansone, S. A., Schultes, E., Sengstag, T., Slater, T., Strawn, G., Swertz, M. A., Thompson, M., van der Lei, J., van Mulligen, E., Velterop, J., Waagmeester, A., Wittenburg, P., Wolstencroft, K., Zhao, J., and Mons, B.: The FAIR Guiding Principles for scientific data management and stewardship, Sci. Data, 3, 160018, https://doi.org/10.1038/sdata.2016.18, 2016.

Xiang, L., Schoepfer, S. D., Zhang, H., Cao, C., and Shen, S.: Evolution of primary producers and productivity across the Ediacaran-Cambrian transition, Precambrian Res., 313, 68-77,

https://doi.org/10.1016/j.precamres.2018.05.023, 2018.

Zhang, Q., Bendif, E. M., Zhou, Y., Nevado, B., Shafiee, R., and Rickaby, R. E. M.: Declining metal availability in the Mesozoic seawater reflected in phytoplankton succession, Nat. Geosci., 15, 932-941, https://doi.org/10.1038/s41561-022-01053-7, 2022.

Zhao, K., Zhu, G., Li, T., Chen, Z., and Li, S.: Fluctuations of continental chemical weathering control primary productivity and redox conditions during the Earliest Cambrian, Geol. J., 58, 3659-3672, https://doi.org/3659-3672, 10.1002/gj.4778, 2023.